

# Operating Pressure Sensitivity of Distillation—Control Structure Consequences

Hong Wen Li, Torben Ravn Andersen, Rafiqul Gani, and Sten Bay Jørgensen\*

*Department of Chemical Engineering, Technical University of Denmark, DK 2800 Lyngby, Denmark*

The influence of pressure variations upon distillation operation does not seem to be well-understood in the open literature, because contradicting statements concerning the importance of pressure control on binary distillation are found. To minimize energy consumption, it is recommended to operate columns at minimum pressure; however, even if column pressure is controlled, instability may still occur when both product purities are controlled in a decentralized control structure. In this paper, operating pressure sensitivity is classified according to the pressure sensitivity of the vapor–liquid equilibrium (VLE) relationship for the mixture being separated. Operating pressure sensitivity is shown to become significant at high internal flow rates. It is furthermore shown that this sensitivity may lead to a situation where different values of the internal flow rate may produce the same product purity, which commonly is labeled “input multiplicity” of the separation. This input multiplicity is shown to occur through a theoretical analysis combined with simulation of the case study and an extended series of experiments. The input multiplicity can be explained by two opposing effects from varying internal flows: the first comes from the well-understood effect of changing the slope of the operating lines, whereas the second is due to the effect of pressure on the VLE relationship. Understanding the input multiplicity or, rather, the pressure sensitivity is relevant for efficient exploitation of the separation capacity of the column through proper control structure selection, i.e., for determination of where to place sensors in a distillation column for controlling pressure. It is shown that the distillation column is most efficiently utilized by controlling the pressure at the column bottom/top for a negative/positive-pressure-sensitive mixture. It is furthermore concluded that controlling the column pressure at the proper end of the column may be crucial to column stability when both product purities are controlled in a decentralized control structure. In an experimental verification, it is demonstrated that, for separating a mildly negative-pressure-sensitive mixture, the distillation column separation capacity is most efficiently exploited when controlling the column pressure at the bottom of the distillation column. For the investigated mixture, it is shown that a 20% higher capacity may be obtained at a lower energy requirement. Thus, a significantly (20%) lower energy expenditure per produced unit is realized through the improved control structure, when compared to conventional control of the column pressure at the top of the distillation column.

## 1. Introduction

Distillation is, by far, the most widely used industrial separation technique. To ensure reliable operation of distillation columns, many variables must be controlled ideally through application of a suitable control structure where different measurements are paired with relevant actuators. Among the variables to be controlled, column pressure is most often listed. The design pressure for distillation is usually determined through analysis of the possibilities for process integration, i.e., to ensure the most efficient exploitation of the available process integration potential. Thus, pressure sensitivity is being exploited regularly in the design of distillation sequences, such as in the Linde column system, where distillation at two different pressures is used to achieve thermal integration and also to circumvent azeotropic distillation by, e.g., increasing the pressure. However, as already stated by Chin,<sup>1</sup> there is a need for a better understanding of distillation pressure control. However, little attention has been given to distillation column operating pressure sensitivity in the otherwise vast literature on distillation dynamics (see the works of Tolliver and Waggoner<sup>2</sup> and Skogestad<sup>3</sup>). Buckley, Luyben, and Shunta<sup>4</sup> claimed that most columns do not need tight pressure control and that sometimes it may even be undesirable, because sudden changes in column pressure (presumably induced by the operator) may result in either flooding or weeping. On the other hand, both Shinskey<sup>5</sup> and Deshpande<sup>6</sup> state that column pressure should be controlled

to avoid sudden increases or decreases in pressure, which could result in flooding or weeping if the column is operated near these limits. In addition, they state that pressure should be constant, such that temperatures can be used to infer composition and because pressure significantly affects the separation capability of the column. However, Shinskey<sup>5</sup> also suggested the operation of distillation columns with a floating pressure to enable minimizing the pressure to minimizing energy expenditure. It must be noted that Shinskey<sup>5</sup> also remarked that this scheme cannot be recommended for certain plants without being more specific.

Column pressure should clearly be observed and controlled carefully when operating near flooding or weeping limits, as noted previously. This statement is valid for columns operated both with and without composition control. In the following, however, it is shown that tight control of column pressure may be desirable, regardless of the closeness to flooding or weeping limits. The reason for this necessity is that the relative volatility of the components may be sensitive to pressure. And, because the column actuators affect both the column pressure as well as the internal flow rates, the column separation capability may be more effectively exploited if pressure is controlled in the proper column end, dependent on the pressure sensitivity of the mixture being separated.

The purpose of this paper is to investigate the sensitivity of distillation performance to operating pressure. The implication of this sensitivity on control structure selection is investigated. First, pressure sensitivity for a mixture to be separated is defined. An analysis of pressure sensitivity of distillation performance

\* To whom all correspondence should be addressed. Tel. +45-45252872. Fax: +45 45932906. E-mail address: sbj@kt.dtu.dk.

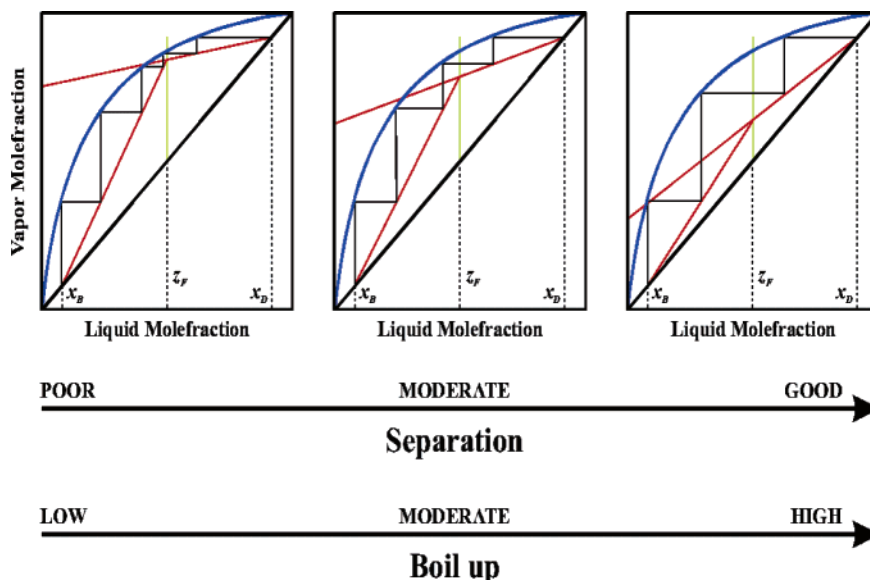


Figure 1. Boilup affects the slopes of the operating lines visualized in a McCabe–Thiele diagram.

then is presented. Here, it is argued that, for certain mixtures, input multiplicity may result at high internal flow rates. An experimental pilot plant is presented where the input multiplicity is, first, analyzed using simulation and then demonstrated during extensive experiments. The implications of pressure sensitivity on control structure selection is analyzed and also demonstrated experimentally. The consequence of controlling pressure in the proper end of a distillation column is shown to be a higher capacity and better utilization of the separation potential in the column.

## 2. Methods

**2.1. Classification of Operating Pressure Sensitivity.** Distillation performance is sensitive to the operating pressure. This sensitivity may be investigated through evaluation of the separation factor, which for a binary zeotropic mixture is defined as

$$S = \frac{y_D/(1 - y_D)}{x_B/(1 - x_B)}$$

For pressure-sensitive mixtures, assuming that constant relative volatility applies, then two main types of pressure sensitivity may be defined: a mixture that has  $\partial\alpha/\partial P < 0$  is said to exhibit negative pressure sensitivity, whereas a mixture with  $\partial\alpha/\partial P > 0$  exhibits positive pressure sensitivity. For a negative-pressure-sensitive mixture, when the pressure increases, the separation factor decreases; for the positive-pressure-sensitive mixture, the separation factor increases when the pressure increases. It will later be shown that, for these two types of systems, different decentralized control structures should be used to control pressure to exploit the column separation capability most efficiently. In regard to the occurrence of the two types of pressure sensitivity, most of almost-ideal separations belong to the negative-pressure-sensitive type. However, it is interesting to note that if a system has a pressure-sensitive azeotrope, then both of the previously mentioned two types of pressure sensitivity can be relevant, with one on each side of the azeotropic point in the equilibrium diagram until the azeotrope disappears at some pressure. Thus, which dependence will be present in a distillation column is dependent on the feed composition, relative to the azeotropic composition. Examples

of such systems are ethanol–water and 2-propanol–water, where the azeotrope disappears at higher pressure than atmospheric pressure, but with lower relative volatility than that present at lower pressures.

**2.2. Systematic Model Analysis.** The operating pressure affects the separation factor as presented previously. At the same time, other variables affect the separation factor, in particular, the boil-up flow rate. For a negative-pressure-sensitive system, where separation improves as the pressure decreases, assuming that the column pressure is allowed to float, then an increase in the heat input to the reboiler (keeping all other inputs constant) results in two opposing effects. The effect of slope sensitivity of the operating line may be visualized in a McCabe–Thiele diagram, to give better separation, as illustrated in Figure 1.<sup>7</sup> This figure shows that a saturated liquid feed mixture of composition  $z_F$  is separated into two products, of composition  $x_D$  and  $x_B$ . As the vapor flow rate is gradually increased, the slopes of the operating lines approach the diagonal, thus resulting in fewer ideal equilibrium stages necessary to obtain the specified purities. The second effect of equilibrium curve sensitivity is that of increased pressure, because of higher internal flow rates, which, for negative-pressure-sensitive mixtures (including the one investigated experimentally below), flattens the equilibrium curve. This second effect yields a more difficult separation as the relative volatility is decreased for the case illustrated in Figure 2.

At low-to-moderate vapor flow rates, an increase in the heat input to the reboiler will give better separation, because the operating line sensitivity is dominating. However, in search for still-higher bottom purity, a point will be reached where the operating line is not improved significantly while column pressure is increased. The equilibrium curve sensitivity may then dominate the operating slope sensitivity, such that the separation factor decreases as the internal flow rate increases for a negative-pressure-sensitive mixture. Hence, for two different internal flow rates located on either side of the maximum separation, the same separation factor (or purity) may be achieved, thus leading to input multiplicity, i.e., that the same output property (here, the separation factor) may be achieved for different values of the input, i.e., the reflux flow rate.

The aforementioned analysis was conducted for the separation factor, simply because this is most directly compared if a column is operated with a fixed concentration somewhere along the

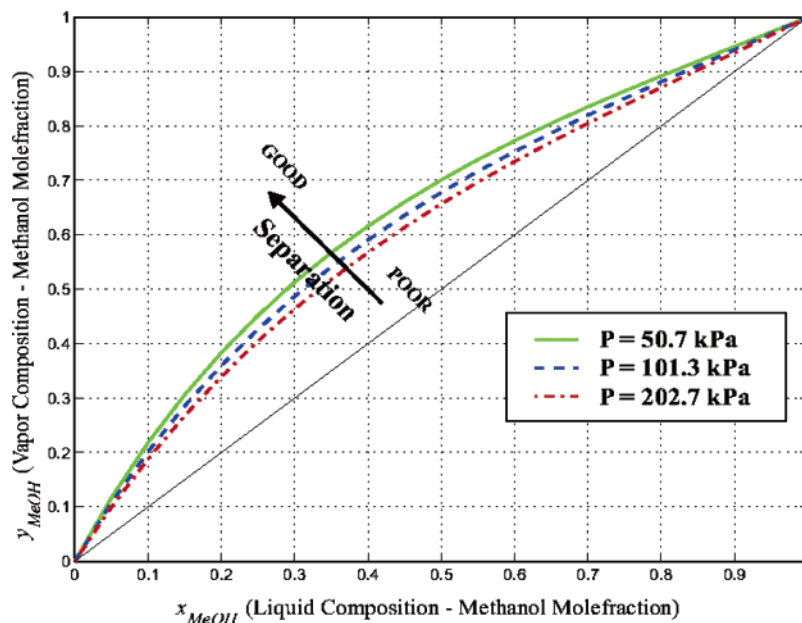


Figure 2. Pressure effect on the vapor-liquid equilibrium (VLE) of the methanol-2-propanol system.

column length. However, the dependence of the top (or bottom) purity would be similar to what is shown for the separation factor previously mentioned. Following the same arguments as those for the separation factor, then the top purity dependence of an increasing reflux flow rate will be an increasing function until the working line is almost diagonal; then, the pressure effect will start to dominate for further increasing reflux flow rate, which, for a negative-pressure-sensitive mixture, will lead to a decreasing top purity. These two effects, in combination, mean that the first term in the sensitivity factor,  $y_D/(1 - y_D)$  is a convex function of the reflux flow rate. Similarly, the second term in  $S$  also will be a convex function of the reflux flow rate. Because the product of two convex functions also is convex, the separation factor indeed is a convex function of the reflux flow rate. This means that if an input multiplicity occurs in the purity, then this also will be the case for the separation factor. However, the location of the maximum separation factor, compared to the maximal purity, will be dependent on the particular separation. This may be illustrated by differentiating the separation factor, with respect to the molar reflux flow rate:

$$\frac{\partial S}{\partial L_M} = \frac{1 - x_B}{(1 - y_D)^2 x_B} \frac{\partial y_D}{\partial L_M} + \frac{y_D}{x_B^2 (1 - y_D)} \left( - \frac{\partial x_B}{\partial L_M} \right) \quad (1)$$

Thus, only for a symmetric separation where the two purity derivatives are numerically equal will the location of the maximum separation factor ( $\partial S/\partial L = 0$ ) and the purity maxima coincide. For nonsymmetric separations, the maximal separation factor will lie between those of the two purity extrema. The precise location of the maximum separation factor is dependent on the properties of the separation and on the pressure profile imposed on the column through the selected operation policy. This aspect will be studied further, using simulation of the specific case study.

### 2.3. Description of Experimental Distillation Pilot Plant.

Figure 3 shows the flowsheet of an indirect vapor recompression distillation pilot plant (IVaRDIP) suitable for separating a mixture of methanol and 2-propanol with a small amount of water impurity. The plant consists of a distillation column, a thermosiphon reboiler, a total condenser, and a reflux drum. The 0.45-m diameter column has 19 sieve trays with 8-mm

holes. To reduce energy consumption, the reboiler and condenser are energy-integrated through a heat pump. The experimental facility is located at the Department of Chemical Engineering at the Technical University of Denmark.

PT100 temperature sensors are located in the gas-liquid spray on trays 1, 5, 10, 15, and 19. In combination with pressure measurements (located in the column bottom, on tray 10 and in the column top), the temperature measurements are suited for concentration estimates. All flows in and out of the system and the reflux flow rate are measured on a mass basis, using Coriolis flowmeters from experiment II and onward. Feed, bottom product, and distillate are sampled manually at each steady state for later gas chromatographic analysis.

The heat pump has an expansion valve (Exp. Valve) that throttles high-pressure liquid heat pump fluid to a lower pressure ( $P_L$ ) suitable for evaporation in the condenser, which, on the heat pump side, works as a flooded boiler, using the flow rate through the expansion valve as an actuator in a mechanical level control loop. After the condenser, there is a control valve (CV9) by which the heat pump fluid vapor flow rate can be manipulated. After superheating the vapor, the compressor elevates the pressure to a higher value ( $P_H$ ) that is suitable for condensation in the reboiler. A small part of the condensation occurs in a secondary condenser, which, using a cooling water circuit, is connected to a set of air coolers. The cooling rate can be manipulated by the control valve CV8, which is thus used to control  $P_H$ . Through the storage tank (Rec) and the superheater heat exchanger, the heat pump fluid circuit is closed at the expansion valve.

The additional basic control loops are as follows. The accumulator level is controlled by the reflux flow rate  $L$ , and the reboiler level is controlled by the bottom product flow rate  $B$ . The column pressure and column vapor flow rate are controlled by a multivariable control (MIMOSC), which coordinates the two heat-pump pressure-control-loop setpoints  $P_{L,set}$  and  $P_{H,set}$ . The concentration profile is retained in the column by maintaining the estimated composition on tray 15 at  $x_{15} = 0.75$  by manipulating the distillate flow rate  $D$ .

**2.4. Pressure Sensitivity.** The pressure sensitivity of a distillation column may be analyzed through simulation where different pressure profiles are induced using a particular

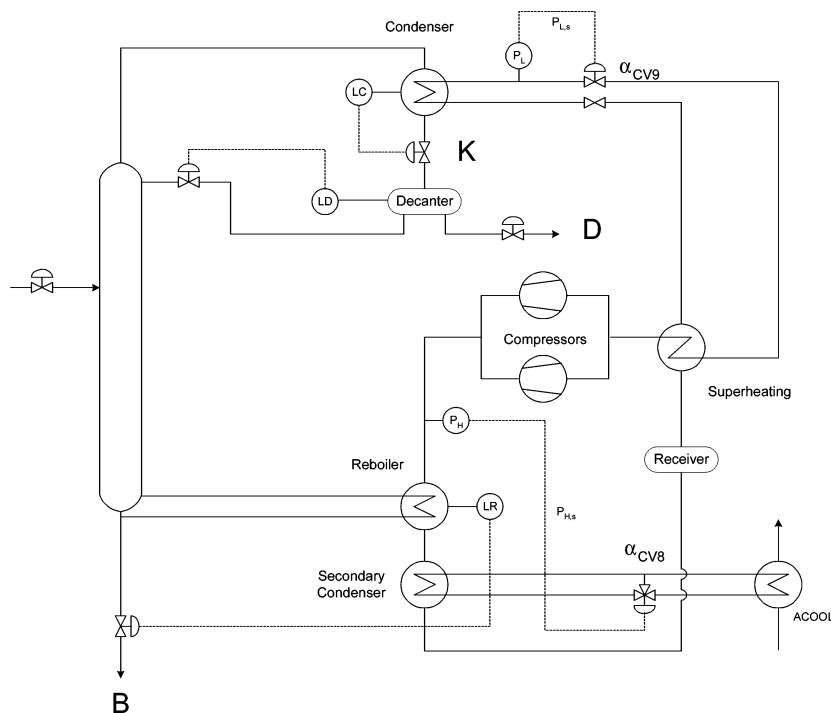


Figure 3. Flow sheet for the indirect vapor recompression distillation pilot plant (IVaRDIP), including basic control loops.

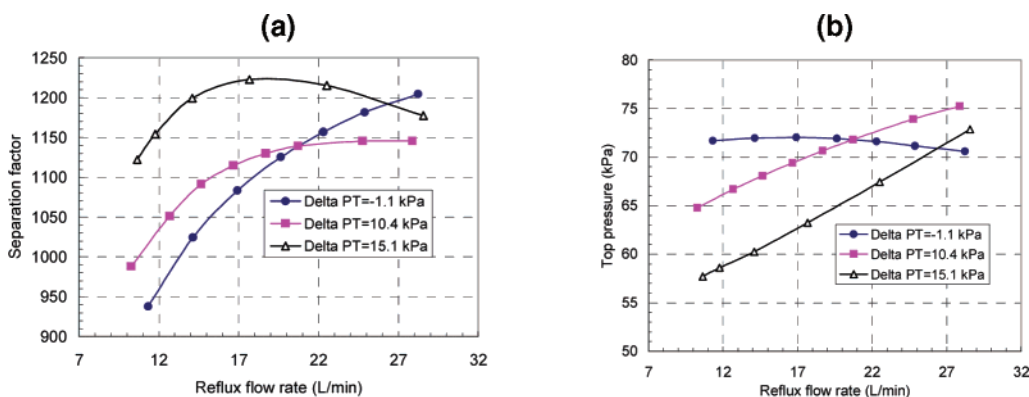


Figure 4. (a) Dependence of the separation factor of the reflux flow rate for three imposed operating pressure dependences. (b) Top pressure as a function of the reflux flow rate for the three cases.

operating policy, e.g., through control. An investigation to illuminate this point is performed for the IVaRDIP and is illustrated in Figure 4, using the model of Li et al.,<sup>8</sup> where different pressure profiles are imposed through the column operation policy. On the IVaRDIP, different column pressure profiles are imposed through the selection of suitable combinations of  $P_{L,set}$  and  $P_{H,set}$  with the level control loops closed. Thereby, the reflux flow rate is increased as shown in Figure 4, while the top pressure is varied in the three cases as shown in Figure 4b with different top pressure relations to reflux flow rate given as delta PT over the reflux flow range. Thus, the top pressure is kept almost constant, increases with 10 kPa and with 15 kPa as the reflux flow rate is increased from 10 L/min to 28 L/min. Figure 4a clearly shows that, as the operating pressure is increased, the separation factor for the simulated case develops a maximum around a reflux flow rate of 18–20 L/min, thereby revealing the possibility for the occurrence of input multiplicity. The investigation reveals that the selection of a control strategy for column pressure may have significant impact on the possible occurrence of input multiplicity of the separation factor.

The temperature profile in a distillation column is closely related to the pressure profile. For the IVaRDIP, this relationship in the almost binary distillation column may be illustrated using

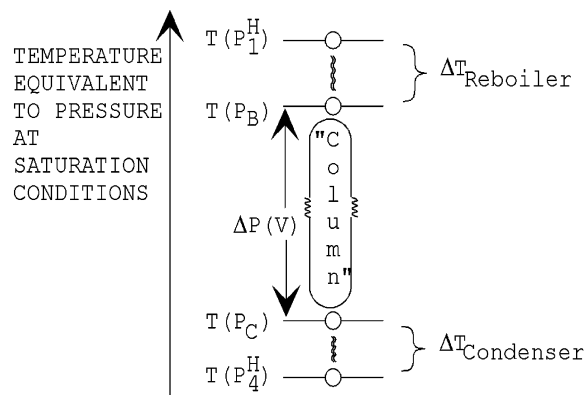


Figure 5. Illustration of the heat-integrated distillation pilot plant (IVaRDIP) pressure-temperature relationship on a mechanical analogue.

the elastic mechanical analogue shown in Figure 5.<sup>9</sup> Here, the column is balanced between temperatures that correspond to the selected heat-pump pressures  $P_{L,set} = P_4^H$  and  $P_{H,set} = P_1^H$ . The vertical location of the column in this analogy represents the column pressure in the reboiler ( $P_B$ ) and the condenser ( $P_C$ ), designated by their corresponding saturation temperatures for

the almost-pure products. The vertical column length represents the pressure drop, which is strongly dependent on the vapor flow rate,  $V$ . The temperature differences over the reboiler and condenser multiplied by their effective heat-transfer rates and areas must be balanced at steady state. This analogy clearly depicts that, if both heat-pump pressures are increased, the column pressure then increases, whereas if the difference between the two heat-pump pressures is increased, the vapor flow rate then is increased instead, resulting in a higher pressure drop over the column. These relationships are explored further in the model analysis of Li et al.<sup>8</sup> In the present context, the mechanical analogue illustrates that there may indeed be a difference between fixing the column pressure either in the reboiler or in the condenser.

Because the flow rates are measured accurately on a mass basis, it may be questioned which static relationship is being investigated when a zero of the separation factor (or top purity) transfer function to reflux flow rate is investigated. To elucidate this question further, the relationship is derived below between the top purity transfer function from mass reflux flow rate ( $dy_D/dL$ ) and the top purity from molar reflux flow rate ( $dy_D/dL_M$ ) at steady state. It is assumed that the bottoms and distillate flow rates remain constant as the boil-up reflux flow rates are changed. Thus,

$$\begin{aligned} \left(\frac{\partial y_D}{\partial L}\right)_p^0 &= \left(\frac{\partial y_D}{\partial L_M}\right)_p^0 \frac{dL_M}{dL} \\ &= \left(\frac{\partial y_D}{\partial L_M}\right)_p^0 \left(M_T - L_M(M_2 - M_1) \left(\frac{\partial y_D}{\partial L_M}\right)_p^0\right)^{-1} \end{aligned} \quad (2)$$

where the relationship between the molar and mass reflux flow rate,  $L = L_M M_T$ , is derived from the molar weight of the top composition:  $M_T = y_D M_1 + (1 - y_D) M_2$ . Note that the superscript zero indicates static conditions, whereas the subscript  $p$  indicates constant pressure at a specified location in the column.

Hence, a static zero of the mass-based reflux flow rate is closely related to the location of a static zero of the molar based transfer. A similar result can be obtained for the bottom purity. Thus, the separation factor sensitivity in eq 2 can be expressed for the static case with the mass flow rates:

$$\begin{aligned} \left(\frac{\partial S}{\partial L}\right)_p^0 &= \left(\frac{\partial S}{\partial L_M}\right)_p^0 \left(\frac{dL_M}{dL}\right) \\ &= \left(\frac{\partial S}{\partial L_M}\right)_p^0 \left(M_T - L_M(M_2 - M_1) \left(\frac{\partial y_D}{\partial L_M}\right)_p^0\right)^{-1} \end{aligned} \quad (3)$$

Thus, a static zero of the separation factor wrt. the mass flow rate can only be due to a zero of the separation factor wrt. the molar reflux flow rate, because the input transformation does not possess a numerator zero. Thus, it is reasonable, even for this system with large difference in molecular weight of the two components, to investigate the location of a zero using mass-based flow rates.

**2.5. Control Implications.** From the analysis of operating pressure sensitivity in sections 2.2 and 2.4 previously discussed, input multiplicity may occur at high internal flow rates. Thus, it is desirable to discuss how to control the system with a possible input multiplicity. Based on the discussion of potential problems related to operation with floating pressure, one may decide that it would be reasonable to have column pressure under feedback control. However, as illustrated in section 2.4, above "column pressure" is an ambiguous phrase, because the

**Table 1. Feed-Flow-Rate Set Points for the Four Experiments**

| experiment | feed-flow-rate set point (ton/h) |
|------------|----------------------------------|
| I          | 0.066 ± 0.0004                   |
| II         | 0.070 ± 0.0009                   |
| III        | 0.110 ± 0.0002                   |
| IV         | 0.12 ± 0.0004                    |

pressure is not the same on all the trays, and, for conventionally equipped distillation columns, it is not possible to keep the pressure constant on more than one tray when the internal flows change. It is therefore of interest to investigate on which tray it is most desirable to stabilize the column pressure. This issue is analyzed in the following paragraphs.

Let us first assume that, along with the two product purities, the pressure on the top tray or in the condenser is under feedback control. It then would traditionally be expected to be a good idea, if necessary, to use the cooling capacity ( $Q_C$ ) for control of the pressure somewhere near the condenser.<sup>4</sup> For the present example column, this could be performed using the ( $D, P_H$ ) configuration to control the two purities while  $P_L$  is used for column pressure control. Now, if the bottom purity is suddenly decreased due to a disturbance, then the controllers would increase  $P_H$  and decrease  $P_L$  to increase the vapor flow rate while keeping the condenser pressure constant.<sup>9</sup> The increased internal flows enhance the separation and, in this way, the disturbance could be rejected. However, in addition, the increased internal flow rates result in a larger pressure drop across the trays, such that the pressure on the lower trays is increased, because the pressure is controlled at the column top, thereby effectively controlling the top temperature, as illustrated in Figure 5. This increased pressure results, for this negative-pressure-sensitive mixture, in reduced separation capability on these trays. If the internal flow rates are relatively high, the variation of these flows then will have a relatively small direct impact on the separation but a large impact on the pressure drop across each tray. The combination of these effects may result in the dominating effect being that the pressures on the lower trays increase such that the relative volatility is reduced. Thus, control of the top column pressure for a negative-pressure-sensitive mixture is unfavorable for the separation.

Now, let us analyze the process in the same situation but with  $P_L$  used to control the pressure in the reboiler instead. If the bottom purity is decreased due to some disturbance, then, again,  $P_H$  will be increased and  $P_L$  decreased such that the vapor flow rate is increased while now the reboiler pressure is kept almost constant. As previously mentioned, the increased internal flows enhance the separation; however, if these flows are relatively large, this effect may be relatively small. Because of the increased vapor flow rate, the pressure drop across each tray is also increased, as previously mentioned, but because it is now the bottom pressure that is fixed, this increased vapor flow rate results in a reduction of the pressure on all the trays above the reboiler, and this reduction results in a higher relative volatility, such that the separation capability is further improved. Thus, through controlling pressure at the column bottom, the two pressure-sensitivity effects are now both improving the separation. Hence, with control of the bottom pressure, the pressure drop over the trays is exploited, to improve the separation for a negative-pressure-sensitive mixture.

The aforementioned analysis was performed on the IVaRDIP example with the actuators, which are specific for this column. However, the analysis is valid for any column for which boil-up and column pressure are indirectly manipulated by heat input to the reboiler and the cooling rate in the condenser. Thus, the observed properties are indeed valid for the majority of

**Table 2. Static Flow Rates and Power Consumption in Experiment IV with  $F = 0.12 \pm 0.0004$** 

| name | steady-state time (h) | $P_T$ (Top) (kPa) | $P_B$ (Bot) (kPa) | $V$ (m <sup>3</sup> /h) | $F$ (ton/h) | $D$ (ton/h) | $B$ (ton/h) | $L$ (ton/h) | $P\_COW$ (%) |
|------|-----------------------|-------------------|-------------------|-------------------------|-------------|-------------|-------------|-------------|--------------|
| SS1  | 1.5                   | 100               |                   | 1.09                    | 0.12        | 0.035       | 0.085       | 0.827       | 40.9         |
| SS2  | 1.5                   | 100               |                   | 0.981                   | 0.12        | 0.035       | 0.085       | 0.742       | 40.0         |
| SS3  | 1.5                   | 100               |                   | 0.868                   | 0.12        | 0.035       | 0.085       | 0.647       | 38.1         |
| SS4  | 1.5                   | 100               |                   | 0.739                   | 0.12        | 0.035       | 0.085       | 0.552       | 35.1         |
| SS5  | 1.5                   | 100               |                   | 0.661                   | 0.12        | 0.034       | 0.086       | 0.484       | 35.2         |
| SS6  | 1.5                   | 100               |                   | 0.538                   | 0.12        | 0.034       | 0.086       | 0.392       | 33.0         |
| SS7  | 1.5                   |                   | 103               | 0.536                   | 0.12        | 0.034       | 0.086       | 0.390       | 33.7         |
| SS8  | 1.5                   |                   | 103               | 0.660                   | 0.12        | 0.034       | 0.086       | 0.483       | 35.2         |
| SS9  | 1.5                   |                   | 103               | 0.738                   | 0.12        | 0.034       | 0.086       | 0.553       | 35.0         |
| SS10 | 1.5                   |                   | 103               | 0.860                   | 0.12        | 0.034       | 0.086       | 0.646       | 35.9         |
| SS11 | 1.5                   |                   | 103               | 0.979                   | 0.12        | 0.034       | 0.086       | 0.744       | 38.9         |
| SS12 | 1.5                   |                   | 103               | 1.083                   | 0.12        | 0.034       | 0.086       | 0.823       | 39.5         |

distillation columns. Even if the vapor flow is generated by blowing vapor directly into the column base, i.e., no reboiler, the column pressure will still be dependent on this vapor flow rate, because, with constant conditions of the cooling medium, a changed requirement for cooling rate (due to changed vapor rate) can only be met by changing the column pressure and, thereby, the condensation temperature. Hence, for any real distillation column that separates pressure-sensitive mixtures, a conflict between the internal flows and the column pressure potentially exists. The aforementioned analysis first shows that, for such systems operated at higher purities, it is desirable to control column pressure. Second, the analysis further shows that pressure should be controlled at the proper column end, such that the column pressure drop increases will enhance the separation when the internal flow rates increase. That means, for negative-pressure-sensitive mixtures, column pressure should be controlled at the column bottom, whereas for positive-pressure-sensitive mixtures, pressure then should be controlled at the column top. The aforementioned analysis also implies that switching to the desirable control structure from the controlling pressure at the wrong end of the column also will improve the capacity of the distillation column, without seriously affecting the energy expenditure. Alternatively, some of the increased capacity may be traded for a lower energy expenditure to produce to the same specification, because of the improved separation factor.

Finally, the qualitative analysis indicates that synergistically exploiting the effect of the increased pressure drop to improve the separation factor for part of the column when the internal flow rates increase may have a more-pronounced effect on low-pressure separations, where the relative effect of pressure-drop variations will constitute a larger fraction of the total column pressure.

### 3. Experiment

**3.1. Experimental Design.** Four input multiplicity experiments have been performed with increasing feed flow rates, as shown in Table 1. Column top pressure was controlled in part of all experiments. The set point for this loop was 100 kPa. For the fourth experiment, at the end of the top pressure control phase, the pressure control was changed such that the bottom pressure was controlled instead. The composition profiles were fixed at an interior point within the column for all four experiments such that the estimated methanol mole fraction at tray 15, XPTT15, is controlled by manipulating the distillate flow rate ( $D$ ). To eliminate the influence of profile shape, the separation factors were compared for the different experiments.

In all experiments, the on-line data for each operating point were collected. The steady-state measurement means and standard deviations, and the time range specification of the individual steady states, were obtained at these operating points.

The data of experiments I, II, and III, which only had top pressure control structure, are shown in the Appendix. These initial experiments are used for comparison with the results from experiment IV on which the discussion in this paper is focused. The steady-state flow rates and the power consumption obtained during experiment IV are given in Table 2.

The details of four experiments are given below. After startup of the IVaRDIP, the operation entered phase B and phase C, which are distinguished by the column top and bottom pressure control, respectively. For both phases, the liquid levels of the reboiler and accumulator were controlled at constant values. Phase B (described below) was executed in all four experiments, whereas phase C only was executed in experiment IV.

**3.1.1. Phase B: B.1.** Phase A is needed to start the system, and to bring the system to steady state. The multivariable receding horizon controller (MIMOSC) then is activated with set points equal to the process values ( $P_B$ ,  $V_{EST}$ ). The set point to column top pressure is 100 kPa. One-point composition control is activated, with the set point for the mole fraction on tray 15 (XPTT15) equal to 0.75 mol/mol.

**3.1.2. Phase B: B.2.** The initial set point for the boilup is 1.12 m<sup>3</sup>/h.

**3.1.3. Phase B: B.3.** When steady-state conditions have been attained, the column operation is maintained for 1–2 h to collect reliable data for each steady state. Subsequently, samples of the feed and products are collected for subsequent gas chromatographic (GC) analysis. The boil-up flow rate is decreased according to Table 2 (from steady state 1 to steady state 6), given previously, and steady-state conditions are obtained as described previously for each boil-up flow rate.

**3.1.4. Phase C: C.1.** When all steady states in phase B have been obtained, the pressure control scheme is changed, such

**Table 3. Reconciled Compositions**

|              | SS1    | SS2    | SS3    | SS4    | SS5    | SS6    |
|--------------|--------|--------|--------|--------|--------|--------|
| $x_{F,H_2O}$ | 0.0841 | 0.034  | 0.0364 | 0.0322 | 0.0358 | 0.0251 |
| $x_{F,MeOH}$ | 0.4505 | 0.4245 | 0.4257 | 0.4277 | 0.4186 | 0.4247 |
| $x_{F,PrOH}$ | 0.4654 | 0.5415 | 0.5379 | 0.5401 | 0.5455 | 0.5501 |
| $x_{D,H_2O}$ | 0      | 0.0017 | 0.0024 | 0      | 0      | 0.0024 |
| $x_{D,MeOH}$ | 0.9731 | 0.9721 | 0.9698 | 0.9736 | 0.9752 | 0.9741 |
| $x_{D,PrOH}$ | 0.0269 | 0.0262 | 0.0277 | 0.0264 | 0.0248 | 0.0236 |
| $x_{B,H_2O}$ | 0.0116 | 0.0316 | 0.0357 | 0.0307 | 0.0368 | 0.0297 |
| $x_{B,MeOH}$ | 0.0563 | 0.0342 | 0.0323 | 0.0298 | 0.0292 | 0.0417 |
| $x_{B,PrOH}$ | 0.9321 | 0.9342 | 0.932  | 0.9395 | 0.934  | 0.9287 |
|              | SS7    | SS8    | SS9    | SS10   | SS11   | SS12   |
| $x_{F,H_2O}$ | 0.0318 | 0.0321 | 0.0329 | 0.0331 | 0.0296 | 0.0284 |
| $x_{F,MeOH}$ | 0.4227 | 0.4184 | 0.4176 | 0.4184 | 0.4196 | 0.4177 |
| $x_{F,PrOH}$ | 0.5455 | 0.5495 | 0.5496 | 0.5485 | 0.5508 | 0.5539 |
| $x_{D,H_2O}$ | 0      | 0.0021 | 0.0024 | 0.002  | 0.0012 | 0.0025 |
| $x_{D,MeOH}$ | 0.9766 | 0.9728 | 0.9709 | 0.971  | 0.973  | 0.9716 |
| $x_{D,PrOH}$ | 0.0234 | 0.0251 | 0.0267 | 0.0269 | 0.0259 | 0.0259 |
| $x_{B,H_2O}$ | 0.0264 | 0.033  | 0.0372 | 0.0318 | 0.0673 | 0.0379 |
| $x_{B,MeOH}$ | 0.0414 | 0.0284 | 0.029  | 0.031  | 0.0372 | 0.0365 |
| $x_{B,PrOH}$ | 0.9322 | 0.9386 | 0.9338 | 0.9372 | 0.8955 | 0.9257 |

that MIMOSC controls the column bottom pressure. The set point for the column bottom pressure is set equal to the actual measurement of the column bottom pressure at the last obtained steady state (where  $V_{SET} = 0.52 \text{ m}^3/\text{h}$ ), i.e., 103 kPa.

**3.1.5. Phase C: C.2.** The boil-up flow rate is then increased stepwise again, as shown in Table 2 (steady states 7–12), and steady-state conditions are obtained for each boil-up flow rate. After each set of steady-state conditions has been attained, samples of the feed and products are collected and analyzed as noted previously.

**3.2. Data Reconciliation.** To obtain consistent data sets, the results from the GC analysis and the online external flow measurements from the experiments were reconciled. This is done to ensure that the overall mass and component balances are achieved at a steady state.

The objective function for the measurements for the data reconciliation is

$$F_{\text{Obj}} = \sum_i \left( \frac{y_i^m - y_i^f}{\sigma_i} \right)^2 \quad (4)$$

where  $y_i^m$  is the measured value,  $y_i^f$  is the calculated fitted value, and  $\sigma_i$  is the standard deviation of measurement  $i$ . The measured variables  $y_i^m$  are feed, top, and bottom compositions, and external flow rates, as follows:

$$y^m = [x_{F,H_2O} x_{F,MeOH} x_{F,PrOH} x_{D,H_2O} x_{D,MeOH} x_{D,PrOH} x_{B,H_2O} x_{B,MeOH} x_{B,PrOH} F D B]^T \quad (5)$$

The static balances and constraints are

$$0 = F - D - B \quad (6)$$

$$0 = F_M x_{F,MeOH} - D_M x_{D,MeOH} - B_M x_{B,MeOH} \quad (7)$$

$$0 = F_M x_{F,PrOH} - D_M x_{D,PrOH} - B_M x_{B,PrOH} \quad (8)$$

$$0 \leq x_{k,j} \leq 1 \quad (9)$$

$$\sum_j^3 x_{k,j} = 1 \quad (10)$$

$$0 \leq F \leq F_{\text{Feed}} \quad (11)$$

$$0 \leq D \leq F_{\text{Feed}} \quad (12)$$

$$0 \leq B \leq F_{\text{Feed}} \quad (13)$$

The aforementioned objective function (eq 1) was minimized to determine  $y_i^f$ .

The standard deviation for each composition measurement is determined from the measured GC results:

$$\sigma = [\sigma_{F,xH_2O} \sigma_{F,xMeOH} \sigma_{F,xPrOH} \sigma_{D,xH_2O} \sigma_{D,xMeOH} \sigma_{D,xPrOH} \sigma_{B,xH_2O} \sigma_{B,xMeOH} \sigma_{B,xPrOH} \sigma_F \sigma_D \sigma_B] \\ = \begin{bmatrix} 0.0018 & 0.006924 & 0.005825 & 0.001869 & 0.002225 & 0.001338 \\ 0.001857 & 0.005209 & 0.005068 & 0.000614 & 0.00068 & 0.004578 \end{bmatrix} \quad (14)$$

The reconciliated composition data for each state are listed in Table 3. With the reconciliated composition data, the inherent separation factors are calculated for each steady state.

Figure 6 shows the vapor flow rate in the column during the entire B and C phases of experiment IV. The steady-state

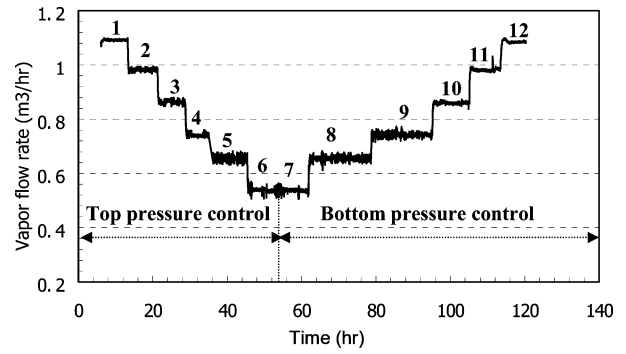


Figure 6. Vapor flow rate during experiment IV.

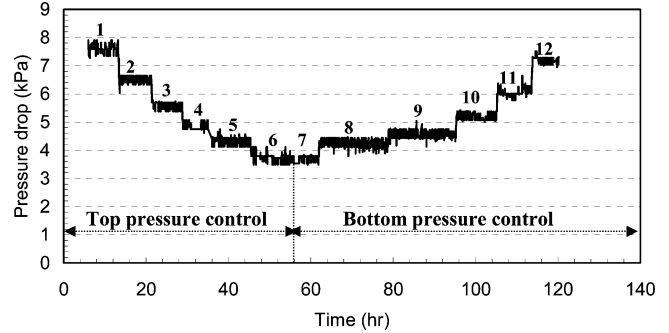


Figure 7. Pressure drop over the column during experiment IV.

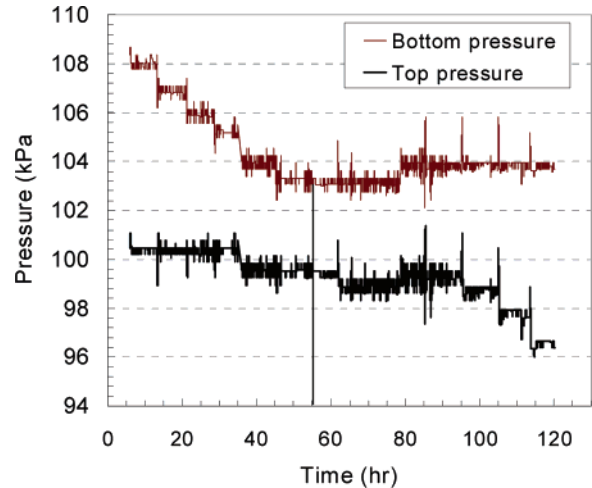


Figure 8. Unfiltered values of distillation column bottom and top pressure during experiment IV.

number, top pressure and bottom pressure controlled, and the set of vapor flow rates are listed in Table 2. It can be seen that, from steady state 1 to steady state 6, the column was top-pressure-controlled from 6 h to 56 h and from steady states 7–12, the column was switched to bottom pressure control from time 56 h to 120 h.

#### 4. Experimental Results and Discussion

The column pressure drop, and the top and bottom pressures, during experiment IV are shown in Figures 7 and 8, respectively. Figure 9 shows the pressure drop versus the reflux flow rate. With the selected pressure set points, the mean column pressure was ~102 kPa during top pressure control and ~100.5 kPa during bottom pressure control.

**4.1. Inherent Separation Factor. 4.1.1. Control of Column Top Pressure.** The separation factors for column top pressure control are shown in Figure 10. This figure shows that an input

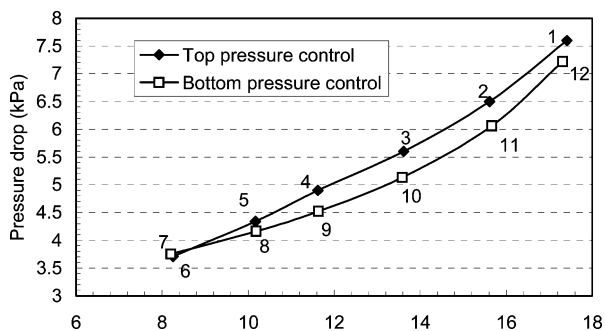


**Figure 9.** Pressure drop versus reflux flow rate for steady-state experiment IV.

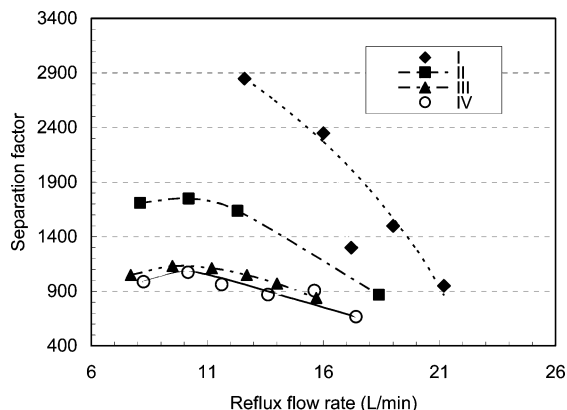


**Figure 10.** Inherent separation factor versus reflux flow rate with top pressure control for the four input multiplicity experiments.

multiplicity becomes more and clear as the feed flow increased from 0.066 ton/h to 0.12 ton/h. This result validates the theoretical analysis, i.e., the separation factor can be viewed as consisting of two contributions of different signs; the first one comes from the well-understood effect of changing the slope of the operating lines, whereas the second is due to the effect of pressure on the equilibrium curve. The contribution from the equilibrium curve sensitivity will, in most cases, be insignificant at low internal flow rates. Thus, at low internal flow rates, the operating line sensitivity is the dominating effect, i.e., when the reflux flow rate increases, the separation factor increases. However, the increased internal flow rate will increase the column pressure and thus reduce the separation capability for the negative pressure sensitivity of the present separation mixture. When the internal flow rates increase, the column pressure reaches such a value that it may bring the plant to a situation where the two contributions are of equal magnitude, i.e., where maximum separation is achieved. After the maximum separation, the pressure effect, with control of column pressure at the column top, as well as entrainment may have a significant role in reducing the separation factor. Thus, increasing the internal flow rate further will decrease the separation factor, as clearly observed at the high internal flow rates in Figure 10.

**4.1.2. Control of Column Bottom Pressure.** An ~5% higher maximal separation factor is obtained with bottom pressure control, as shown in Figure 11, when compared to top pressure control at approximately the same mean column pressure. Furthermore, the maximal separation factor is obtained at a ~20% higher internal flow rate than that with column top pressure control. From Table 2, it is noted that the energy expenditure for operation at steady state 9 versus steady state 4 are approximately the same, as also observed in Figure 12. Thus, this finding validates that the column is more efficiently utilized with control of column bottom pressure when separating a negative-pressure-sensitive mixture.

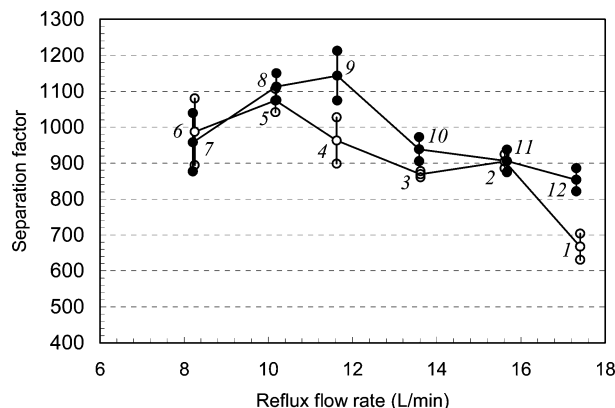


**Figure 11.** Inherent separation factor with standard deviation versus reflux flow rate, relative to both top pressure and bottom pressure control, for experiment IV. Steady states 1–6 have top pressure control, whereas steady states 7–12 have bottom pressure control.

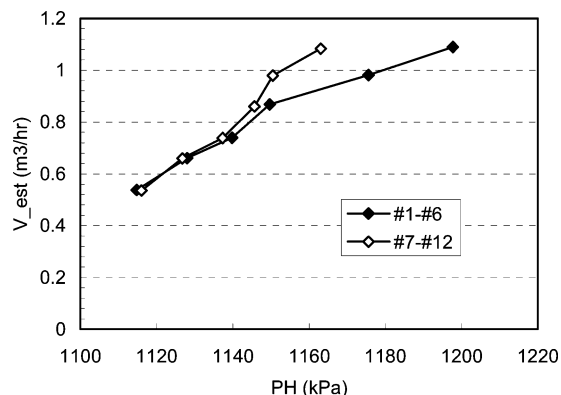


**Figure 12.** Vapor flow rate versus heat-pump high pressure: steady states 1–6 have top pressure control, whereas steady states 7–12 have bottom pressure control.

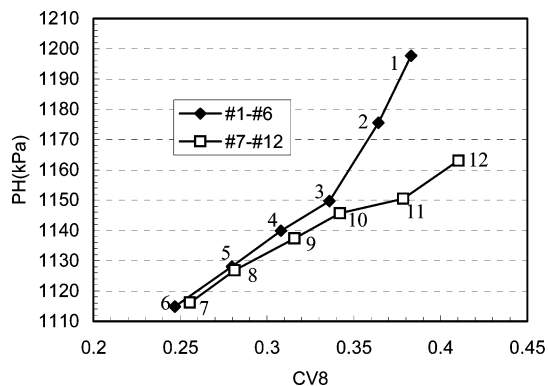


**Figure 13.** Heat-pump high pressure versus control valve CV8: steady states 1–6 have top pressure control, whereas steady states 7–12 have bottom pressure control.

However, it is also clear that both control structures display a maximal separation factor, thereby indicating that entrainment also has a role at high reflux flow rates.

Figures 12 and 13 clearly show that, for the same boil-up flow rate, a lower heat-pump high pressure is needed with the bottom pressure control than with the top pressure control, which means that less energy is needed to achieve the same boil-up rate. The larger opening of CV8 in Figure 13 shows that more energy is cooled away in the air coolers during bottom pressure control.



## 5. Conclusions

Distillation column pressure dynamics is investigated to reveal its influence on distillation column control configuration and column operation efficiency. Phenomenological analysis results reveal a possibility for input multiplicity in a distillation plant. Experiments were conducted on a heat-integrated distillation pilot plant that separated a negative-pressure-sensitive mixture with both top pressure and bottom pressure control structures. The results from these experiments verify the existence of the proposed input multiplicity for a top pressure control structure. For bottom pressure control, a 5% higher maximal separation factor is obtained at a 20% higher internal flow rate at a lower energy requirement. The experimental results thereby confirm that the efficiency of a distillation column that separates a mixture with a pressure-sensitive separation can benefit significantly from the use of the proper pressure control configuration.

The experiment with bottom pressure control also reveals that an input multiplicity exists, even with this most suitable sensor location; this multiplicity is presumably due to entrainment. Controlling column pressure at the proper end of the column also may be crucial to column operating stability when both product purities are controlled in a decentralized control structure since the occurrence of input multiplicity can destabilize a decentralized control structure. For such cases a centralized multivariable control structure with a pressure sensor suitably located according to the mixture pressure sensitivity should be considered.

### Nomenclature

$B$  = flow rate of bottom product (ton/h)  
 $B_M$  = flow rate of bottom product (kmol/h)  
 $CV8$  ( $\alpha_{CV8}$ ) = control valve 8  
 $CV9$  ( $\alpha_{CV9}$ ) = control valve 9  
 $D$  = flow rate of top product (ton/h)  
 $D_M$  = flow rate of top product (kmol/h)  
 $F$  = feed flow rate (ton/h)  
 $F_M$  = feed flow rate (kmol/h)  
 $F_{Obj}$  = object function for data reconciliation  
 $L$  = reflux flow rate (L/min or ton/h)  
 $L_M$  = reflux flow rate (mol/min or kmol/h)  
 $M$  = molecular weight; a subscript T indicates the column top, whereas a subscript 1 or 2 indicates the component number  
 $P$  = column pressure (kPa)  
 $P_T$  = column top pressure (kPa)  
 $P_B$  = column bottom pressure (kPa)  
 $P_L$  (PL) = low pressure on the heat-pump section (kPa)  
 $P_H$  (PH) = high pressure on the heat-pump section (kPa)  
 $Q_C$  = heat duty of the condenser (kJ/h)  
 $Q_B$  = heat duty of the reboiler (kJ/h)  
 $S$  = separation factor  
 $V_{SET}$  = setpoint of vapor flow rate ( $m^3/h$ )  
 $X_{15}$  = methanol mole fraction on tray 15  
 $x_{MeOH}$  = methanol mole fraction in the liquid phase  
 $X_{PTT15}$  = estimated methanol mole fraction on tray 15  
 $x_{B,MeOH}$  =  $x_B$  = methanol mole fraction in the bottom product  
 $x_{B,PrOH}$  = 2-propanol mole fraction in the bottom product  
 $x_{D,MeOH}$  = methanol mole fraction in the top product  
 $x_{D,PrOH}$  = 2-propanol mole fraction in the top product  
 $x_{F,MeOH}$  = methanol mole fraction in the feed product  
 $x_{F,PrOH}$  = 2-propanol mole fraction in the feed product  
 $x_{F,H_2O}$  = water mole fraction in the feed product  
 $y_D$  = methanol mole fraction in the top product

**Table A1. Experiment I with  $F = 0.066 \pm 0.0004$**

| name | steady-state time (h) | $P_T$ (kPa) | $V$ ( $m^3/h$ ) | $F$ (ton/h) | $D$ (ton/h) | $B$ (ton/h) | $L$ (ton/h) |
|------|-----------------------|-------------|-----------------|-------------|-------------|-------------|-------------|
| SS1  | 1.0                   | 100         | 1.378           | 0.066       | 0.02        | 0.046       | 1.089       |
| SS2  | 1.0                   | 100         | 1.28            | 0.066       | 0.02        | 0.046       | 1.011       |
| SS3  | 1.0                   | 100         | 1.13            | 0.066       | 0.02        | 0.046       | 0.893       |
| SS4  | 1.0                   | 100         | 1.029           | 0.066       | 0.02        | 0.046       | 0.813       |
| SS5  | 1.0                   | 100         | 0.9612          | 0.066       | 0.02        | 0.046       | 0.759       |
| SS6  | 1.0                   | 100         | 0.7601          | 0.066       | 0.02        | 0.046       | 0.601       |
| SS7  | 1.0                   | 100         | 0.4627          | 0.066       | 0.02        | 0.046       | 0.366       |

**Table A2. Experiment II with  $F = 0.070 \pm 0.0009$**

| name | steady-state time (h) | $P_T$ (kPa) | $V$ ( $m^3/h$ ) | $F$ (ton/h) | $D$ (ton/h) | $B$ (ton/h) | $L$ (ton/h) |
|------|-----------------------|-------------|-----------------|-------------|-------------|-------------|-------------|
| SS1  | 2.0                   | 100         | 0.5191          | 0.070       | 0.0242      | 0.0434      | 0.386       |
| SS2  | 2.0                   | 100         | 0.766           | 0.070       | 0.0245      | 0.0438      | 0.581       |
| SS3  | 2.0                   | 100         | 0.9825          | 0.070       | 0.0242      | 0.0434      | 0.752       |
| SS4  | 2.0                   | 100         | 101331          | 0.070       | 0.0233      | 0.0456      | 0.872       |
| SS5  | 2.0                   | 100         | 0.6409          | 0.070       | 0.0237      | 0.0445      | 0.483       |
| SS6  | 2.0                   | 100         | 0.416           | 0.070       | 0.0235      | 0.0448      | 0.306       |
| SS7  | 2.0                   | 100         | 0.5152          | 0.070       | 0.0236      | 0.0449      | 0.385       |

**Table A3. Experiment III with  $F = 0.110 \pm 0.0002$**

| name | steady-state time (h) | $P_T$ (kPa) | $V$ ( $m^3/h$ ) | $F$ (ton/h) | $D$ (ton/h) | $B$ (ton/h) | $L$ (ton/h) |
|------|-----------------------|-------------|-----------------|-------------|-------------|-------------|-------------|
| SS1  | 2.0                   | 100         | 0.5152          | 0.11        | 0.035       | 0.075       | 0.373       |
| SS2  | 2.0                   | 100         | 0.6159          | 0.11        | 0.035       | 0.075       | 0.452       |
| SS3  | 2.0                   | 100         | 0.714           | 0.11        | 0.035       | 0.075       | 0.529       |
| SS4  | 2.0                   | 100         | 0.816           | 0.11        | 0.037       | 0.073       | 0.607       |
| SS5  | 2.0                   | 100         | 0.8844          | 0.11        | 0.037       | 0.073       | 0.662       |
| SS6  | 2.0                   | 100         | 0.9841          | 0.11        | 0.037       | 0.073       | 0.741       |
| SS7  | 2.0                   | 100         | 0.812           | 0.11        | 0.037       | 0.073       | 0.604       |
| SS8  | 2.0                   | 100         | 0.5152          | 0.11        | 0.037       | 0.073       | 0.660       |

$y_{MeOH}$  = methanol mole fraction in the vapor phase

$y_i^m$  = measured value

$y_i^f$  = fitted value

$y^m$  = vector of measurement

$\sigma_i$  = standard deviation of measurement  $i$

### Appendix

Tables A1–A3 contain the experimental flow rates for the steady states obtained during experiments I–III.

### Literature Cited

- Chin, T. G.; Guide to distillation pressure control methods. *Hydrocarbon Process.* **1979**, *59*, 145–153.
- Tolliver, T. L.; Waggoner, R. C. Distillation Column Control: A review and perspective from the CPI. *Advances in instrumentation, Proceedings of the ISA Conference and Exhibition 1980*, *35*, 83–106.
- Skogestad, S.; Dynamics and Control of Distillation Columns—A Critical Survey. *IFAC—Symposium DYCORS +92*, College Park, MD, April 27–29, 1992.
- Buckly, P. S.; Luyben, W. L.; Shunta, J. P. *Design of Distillation Column Control System*; Instrumentation Society of America, 1985.
- Shinskey, F. G. *Distillation Control*; McGraw-Hill: New York, 1984.
- Desphande, P. B. *Distillation Dynamics and Column*; Instrumentation Society of America, 1985.
- Andersen, T. R. Optimal Design and Operation of Process Integrated Distillation. Ph.D. Thesis, Technical University of Denmark, Lyngby, Denmark, 2002.
- Li, H. W.; Gani, R.; Jørgensen, S. B. Process Insights-Based Control Structuring of an Integrated Distillation Pilot Plant. *Ind. Eng. Chem. Res.* **2003**, *42*, 4620–4627.
- Koggersbøl, A.; Andersen, B. R.; Nielsen, J. S.; Jørgensen, S. B. Control Configurations for an Energy Integrated Distillation Column. *Comput. Chem. Eng.* **1996**, *20S*, S853–S858.

Received for review January 3, 2006  
 Revised manuscript received July 20, 2006  
 Accepted July 21, 2006